Powder Technology 192 (2009) 33–39

Contents lists available at ScienceDirect

Powder Technology

journal homepage: www.elsevier.com/locate/powtec

Transitions to vibro-fluidization in a deep granular bed

Kenneth J. Ford *, James F. Gilchrist, Hugo S. Caram

Department of Chemical Engineering, Lehigh University, Bethlehem, PA, 18015, USA

ARTICLE INFO

Article history:
Received 18 December 2007
Received in revised form 2 November 2008
Accepted 14 November 2008
Available online 16 December 2008

Keywords:
Granular media
Vibro-fluidization
Quasi-static
Deep granular bed
Vane
granular state
State transitions
Vibration
Power
Torque
Rheology
Hysteresis

ABSTRACT

Granular media subjected to vibration can approximate fluid behavior with sufficient vibration acceleration. Unlike gas fluidization, the transition from a static bed to a liquid-like state is poorly defined and has primarily studied previously in shallow or 2D granular beds. Three granular states are identified in this work: the static, the quasi-static, and the vibro-fluidized state. These states are characterized for a deep granular bed through quantitative measurements of the power or torque required to rotate a vane within the granular media. In this study, the vane is rotated while the bed is subjected to vibration at 10 Hz with acceleration in the range $0 \le \Gamma = \omega^2 x_{max}/g \le 4.0$. We define a critical dimensionless vibration acceleration, Γ_c, based on a dramatic decrease in vane power and the absence of a dynamic zero-shear rate torque, as the transition to vibro-fluidization. Typical of granular materials, significant hysteresis is observed in measuring these bed state transitions. These measurements of "granular rheology" provide a quantitative framework for defining these transitions.

1. Introduction

Considerable recent work has focused on the phase behavior and dynamics of granular materials and significant progress has been made [1]. The lack of constitutive equations to describe phase behavior and kinematics has led to an array of simulation and experimental techniques to determine the granular state [2–5]. This paper focuses on the granular bed phase behavior and kinematics that are of interest to industrial granular processes by adapting a vane shear experimental technique commonly used to test static soil samples to measure the state of a dynamic, vibrated deep granular bed.

For many processes in the pharmaceutical, food/beverage, cosmetic, chemical, petroleum, polymer and ceramic industries, the goal is to achieve or maintain homogeneity of many granular ingredients during processes such as agglomeration, feed stream transport, chemical reactions, coating and others. Knowledge of the granular bed properties and state of the bed is crucial, therefore many experimental methods have been developed including: Bed dilation measurement [6], shear cells [7,8], solid objects moving through the bed [9], couette devices [10–15], and rotating/oscillating rods [16–19] or impellers [20–22] and visual measurements of velocity and segregation [23–29].

The idea of characterizing granular rheology to better understand the behavior of these materials is controversial. While a major effort is underway to derive constitutive equations that describe the kinematics of these materials, there is still a great demand for simple experiments to catalog fundamental granular behavior. The deep granular bed in this paper experiences three phases or granular bed states: The static dense granular state when no granular rearrangement is present, a quasi-static granular state having a finite yield stress or zero shear-rate torque for vibration below a critical dimensionless vibration amplitude, Γ_c, and a vibro-fluidized state above Γ_c. A vane probe is used to measure the granular bed state under dynamic vibrated conditions. The vane was chosen for two reasons. Vanes are common in rheological measurements [30], akin to using cone-and-plate, cup and bob and Couette geometries to isolate the material performance upon deformation. The use of vanes was derived from an existing standard in testing mechanical behavior of soil [31,32] or manufactured food [33–36]. The second reason for choosing a vane probe is its similarity to many industrial granular processing devices, such as those found in pharmaceutical high shear granulators. One can envision partially decoupling the rotational motion and vertical motion to explore various dynamics. When the vane is smaller than the granular bed diameter, as in this paper, the vane can be placed to sample subregions of the bed to probe local behavior.

To date, granular bed vibration research primarily focuses on two dimensional [24,37–40] and three dimensional [25–27,41–46] shallow

* Corresponding author.
E-mail address: kenneth_ford@merck.com (K.J. Ford).

0032-5910/$ – see front matter © 2008 Elsevier B.V. All rights reserved.
doi:10.1016/j.powtec.2008.11.017

granular beds that are only a few particle diameters deep. Shallow beds are of scientific interest because they exhibit complex behavior, such as pattern formation, that result from even a small number of particles. Likewise, limiting the number of particles is convenient for direct simulation using discrete element methods, DEM. However, most industrial granular processes employ beds that are hundreds or thousands of particles deep. For this paper, deep granular beds are defined as those having a depth on the order of hundreds of particle diameters. Industrial examples of deep granular beds include food production blenders, pharmaceutical high shear granulators, particle coaters, cosmetic blenders, fertilizer agglomerators, mining raw material separators, fluidized bed chemical reactors and many others. Design and control of these industrial processes would greatly benefit from a better understanding of the granular states resulting from power input conditions in deep granular beds.

It has long been known that vigorous vibration of a granular bed can lead to vibro-fluidization, a granular state that has some similarities to gas fluidization. Vibro-fluidization causes the granular bed to behave in a fluid manner. The fluidized state is highly desirable in many industrial processes due to the efficiency of mixing/separation, more homogeneous distribution of binder during agglomeration, more homogeneous coating of particles and elimination of species transport limitations in chemical reactors.

Many researchers study vibro-fluidized deep granular beds in one dimension (height only) [28] or in two dimensions, height and width, [47,48] using particle tracking. A few researchers study the affects of vibration on three dimensional deep granular beds. Modeling by Klongboonjit [49] describes the affect of particle elasticity on convection in deep vibrated beds. Rátkai [50], Savage [29] and Sistla et al. [51] each study convective motion in vibro-fluidized deep granular beds using particle tracking. D'Anna et al. [18] and Mayor et al. [19] observe vibro-fluidized "Brownian motion" of a vibrated deep granular bed using a torsion oscillator immersed in the bed. D'Anna and Gremaud [17] use an immersed torsion oscillator to map the bed complex frequency response to vibration and map the bed state. Ehrichs et al. [52], Jaeger et al. [53] and Ehrichs et al. [54] employ magnetic resonance imaging, MRI, to observe deep bed granular convection of vibrated poppy seeds.

Studies that focus on industrially important granular systems tend to employ gas fluidization of granular beds. Gas fluidization alone has a limited ability to reduce agglomerate size, avoid granular bed collapse due to interstitial fluid channeling, and promote homogeneous granular bed fluidization. There are a few examples of agitated gas fluidized systems. Godard and Richardson [55] and Nielsen et al. [56] employ a slowly rotating stirrer, without vibration, to promote homogeneous granular bed fluidization in gas fluidized granular beds. Other researchers have combined gas flow with vibration to promote homogeneous granular bed fluidization. Marring et al. [57] study the effect of vibro/gas fluidization on potato starch beds and report that vibration significantly increases the bed fluidization index, defined as $FI = \Delta pA/mg$. Wank et al. [58], Mawatari et al. [59] and Mawatari et al. [60] study the agglomerate size of vibro/gas bed fluidization. Metcalfe et al. [61] and Tennakoon et al. [62] horizontally vibrate gas fluidized beds and record bed height, dilation. Kuipers et al. [63] maps the fluidization quality for vibro/gas fluidized starch using vane stirring. It should be noted that the onset of fluidization in gas fluidized systems has been well characterized. No such criteria exist for vibro-fluidization, and thus, the characterization of the onset of vibro-fluidization is the primary contribution of this study.

We study the phase behavior of granular systems by rotating a vane probe within a vibrated deep granular bed. The vibration is measured and controlled. The vane probe power draw is measured at various dimensionless vibration acceleration levels, Γ, and vane speeds, Ω, during increase or decrease of each variable. The vibration frequency, f, is held constant at 10 Hz throughout. This research relates to previous studies of vibro-fluidization, however, it focuses on deep granular beds and employs a vane to probe the behavior of the granular bed. As is described below, particle motion within the bed from the vane appears to be confined to the neighborhood of the vane. Likewise, this research is associated with those studies that measure the transition to fluidization, typically performed previously in gas fluidization.

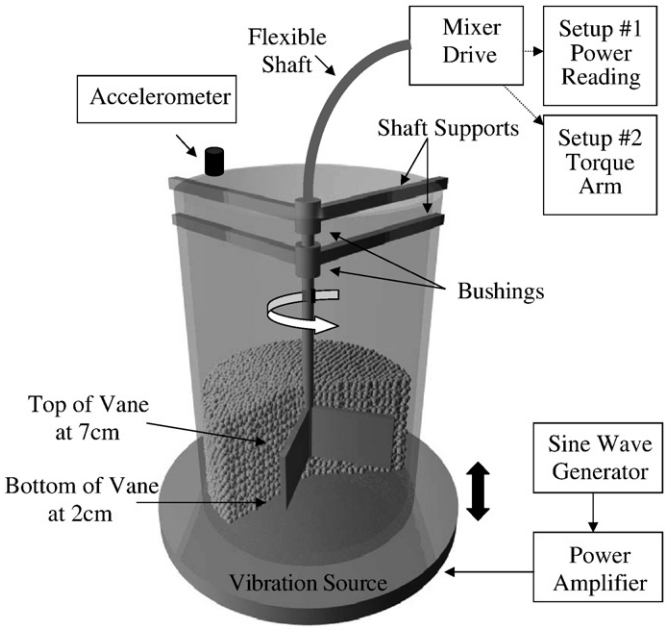

Fig. 1. Schematic of the experimental apparatus.

2. Experimental setup

The experimental setup is illustrated in Fig. 1. A 5.6 cm diameter acrylic column is attached to a vibration source. The column is filled with 150 μm diameter spherical glass beads[1] to a depth of 20 cm (M_B = 754.9 g), approximately 1330 particles deep, in all experiments. A stainless steel 4-blade vane, 3.5 cm diameter × 5 cm tall[2], is attached to the column by bushings on the shaft, so that the vane is in the same vibration reference frame as the column. The vane shaft is driven by two vane setups. Vane setup 1 consists of a drive (Model L1U08, Lightnin, Dublin, Ireland) that directly reports vane power (±0.05 W) and is used for experiments conducted at $200 \le \Omega \le 1000$ rpm. Vane setup 2 consists of a 1/4 hp AC motor (230 V, 1 phase, Reliance Dutymaster, Cleveland, OH) with vane speed, Ω, controlled by a variable speed transmission (Model N29VF, Graham Co., Menononee Falls, WI) mounted on a roller bearing. Torque is measured using a force gauge (pound gauge, Ametek, Hatfield, PA, ±0.005 lb_f) attached to a L = 25.5 cm long torque arm. This vane setup is used for experiments conducted at $20 < \Omega < 120$ rpm. Both drive setups are connected to the vane via flexible shaft to isolate the drive from vibration.

The vibration source is a subwoofer (Model T112D4, Rockford Fosgate, Grand Rapids, MI) driven by a 100 watt amplifier (Model RX-4105, Sherwood America, Cerritos, CA). A signal generator (Model LAG-120B audio generator, Leader, Japan) provides a 10 Hz frequency sine wave signal to the amplifier. The vibration amplitude is measured using an accelerometer (Model 352 C67 accelerometer with a model 480 B power unit, PCB Piezotronics, Depew, NY) that is attached to the top of the column. The accelerometer signal is measured via an oscilloscope (Model TDS 2004B, Tektronix, Beaverton, OR).

Acceleration is controlled by a sinusoidal forcing function, rather than positive displacement. The dimensionless acceleration amplitude is defined as $\Gamma = a_{max}/g$, where a_{max} is the maximum acceleration in the

[1] Average diameter = 154 μm, Median diameter = 152 μm, x_{10} = 99 μm, x_{90} = 203 μm.
[2] Shaft diameter = 7 mm, Blade width = 1.4 cm, Blade thickness = 1 mm.

vertical direction and g is gravity. Since the motion is sinusoidal, the maximum acceleration is related to the maximum displacement by the equation $a_{max}/g=\omega^2 x_{max}/g$,[3] where x_{max} is the maximum displacement from center in the vertical direction. The value for Γ is varied across $0\le\Gamma\le4$ in this study. The vibration frequency, f, is held at 10 Hz throughout this study. For vane setup 1, vane probe power draw, P_{vane}, is read directly from the drive controller. For vane setup 2, P_{vane} is calculated from the torque arm force by $P_{vane}=2\pi\,\Omega\,F\,L/60$, where Ω is the shaft rotation speed in revolutions per minute, F is the force and L is the torque arm length. For vane setup 1, vane probe torque is calculated by $T_{vane}=60\,P_{vane}/2\pi\,\Omega$. For vane setup 2, vane probe torque is calculated by $T_{vane}=F\,L$. Two experimental methods are employed. The vane speed, Ω, is increased/decreased while holding the dimensionless vibration acceleration, Γ, and frequency, f, constant, or the Γ is increased/decreased while holding Ω and f constant.

For $\Gamma\le1$, the granular bed retains contact with the container bottom platform throughout the vibration cycle. At $\Gamma>1$, when the vibration acceleration is larger than gravity, the granular bed has the potential to expand and/or break contact with the platform to take flight during each vibration cycle. Granular bed state changes due to expansion and/or loss of contact with the platform is a primary focus of this paper. At high enough Γ, portions of the granular bed may not return to the previous state prior to the launch time of the next cycle, leading to subharmonic behavior.

It is convenient to non-dimensionalize the vibrating bed vane power using the vane power required when vibration is not present. The dimensionless vane power is defined as:

$$\eta_{vane}=\frac{P_{vane}(vibration)}{P_{vane}(novibration)} \quad (1)$$

A dimensionless vane power of $\eta_{vane}=1$ indicates no effect due to vibration of the granular bed. The lower the value of η_{vane}, the greater the power reduction due to vibration.

Although it would be desirable to use this data to characterized the rheology of the bed, an effective viscosity cannot be derived directly from this data. Kinematic information, such as the depth of the sheared region, cannot be determined directly from these experiments. The shear layer has a depth less than the distance from the vane to the container walls, approximately 70 particle diameters. However, variations in the measured power quantify the general behavior of the system, similar to vane tool measurements characterizing jamming or gelation of a suspension. The affect of bead size, vibration frequency change, column diameter and bed depth will be explored in future studies.

3. Results and discussion

3.1. Power, torque and bed state transitions for increasing Ω

The primary assertion presented is that the granular bed state controls the power required to maintain the vane at a fixed speed within the granular bed. This is shown in Fig. 2 where the vane probe power draw, P_{vane}, is a function of vane speed, Ω, for various dimensionless vibration acceleration, Γ. Note that these measurements are taken for progressively increasing Ω. The data for $\Omega<200$ rpm was taken with vane setup 2, while the data for $\Omega\ge200$ rpm was taken with vane setup 1. Minor data discrepancies between the vane setups are due to equipment differences and small differences in the number of particles contained in granular beds.[4] Three bed states are represented by the data: The static granular state, the quasi-static state and the vibro-fluidized state. For $\Gamma\le1$, the bed is in a static state and vibration has no significant affect on

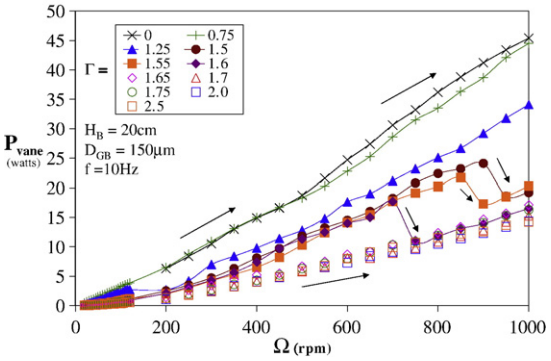

Fig. 2. Vane probe power draw, P_{vane}, for increasing vane speed, Ω - Vibration frequency, f = 10 Hz, particle diameter, $D_{GB}=150$ μm, bed depth, $HB=1330\,D_{GB}$ deep. Three bed states are represented by the data: The static granular state for $0<\Gamma<1$, the quasi-static state for $1<\Gamma<\Gamma_c$ and the vibro-fluidized state for $\Gamma>\Gamma_c$. For $\Gamma\le1$, vibration has no significant affect on the granular bed. When Γ is increased to $1<\Gamma<1.5$, P_{vane} decreases as a strong function of Γ. For $1.5\le\Gamma\le1.6$, Γ reaches a critical point, Γ_c, and a sharp transition to a vibro-fluidized state occurs with increasing Ω. For all experiments where $\Gamma>\Gamma_c$, the bed is vibro-fluidized and P_{vane} is nearly independent of Γ.

the granular bed. In this region, the P_{vane} is highest and is a much weaker function of Γ. When Γ is increased to $1<\Gamma<1.5$, the bed transitions to a quasi-static state where P_{vane} is a strong function of Γ. For each measured profile in the range of $1.5\le\Gamma\le1.6$, Γ reaches a critical point, Γ_c, and a sharp transition to the vibro-fluidized state occurs with increasing Ω. The measured transitions occur with an observable dilation and vibro-fluidization of the bed. After transition to vibro-fluidization, P_{vane} is a much weaker function of Γ. Likewise, for all experiments where $\Gamma>1.6$, the bed is vibro-fluidized and P_{vane} is a much weaker function of Γ.

The only previous work characterizing this transition [6] reports similar transition behavior for shallow beds less than five particle diameters deep vibrated at 4–10 Hz frequency. Using bed expansion measurements, they define a critical acceleration, Γ_c, for transition where the bed suddenly expands. They report that Γ_c is most pronounced for less than a single layer of particles and occurs between $1.5<\Gamma_c<2.0$, the same range as this study. Although their Γ_c is similar to the work in this study, the connection between single bead layers and deep granular beds has not yet been established.

The dimensionless vane power, η_{vane}, is a measure of power reduction due to vibration. Fig. 3 shows the dimensionless vane power, η_{vane}, as a function of vane speed, Ω, for various dimensionless vibration accelerations, Γ. The η_{vane} graph demonstrates the same characteristic behaviors as P_{vane} in Fig. 2 with $\eta_{vane}\approx1$ indicating no effect of vibration and $\eta_{vane}<1$ indicating the extent of vibration effect.

Fig. 3 also demonstrates that for constant Γ, η_{vane} is a much weaker function of Ω for $\Omega>500$ rpm, except during bed state transition. This indicates that the Ω contribution to bed agitation cancels out. Fig. 4 shows the average η_{vane} for each Γ at $\Omega>500$ rpm vs. Γ. The quasi-static and vibro-fluidized bed states demonstrate the same behaviors for average η_{vane} vs. Γ that were previously shown for η_{vane} vs. Ω. The quasi-static state demonstrates average $\eta_{vane}\approx1$ for $\Gamma<1$ while the average η_{vane} decreases as a strong function of Γ for $1<\Gamma<1.5$. Transitions to the vibro-fluidized state occur in the range of $1.5\le\Gamma_c\le1.6$, demonstrated by sudden drop in average η_{vane}. The vibro-fluidized state occurs for $\Gamma>\Gamma_c$ where the average η_{vane} is lowest and a much weaker function of Γ.

Vane torque data is shown in Fig. 5. The same general observations found in the behavior of P_{vane} exist. The highest torques are observed for the quasi-static state where $\Gamma<1$, torque is a strong function of Γ for $1<\Gamma<\Gamma_c$, bed state transitions occur within the range of $1.5\le\Gamma\le1.6$, and common power and torque behavior are found for the vibro-fluidized bed state where $\Gamma>\Gamma_c$. For most granular flow models, the torque would be independent of the angular velocity. The authors speculate

[3] Note: $\omega=\frac{2\pi f}{60}$.

[4] Each vane setup required a new granular bed pour into the column. The number of particles in the bed was controlled by mass measurement.

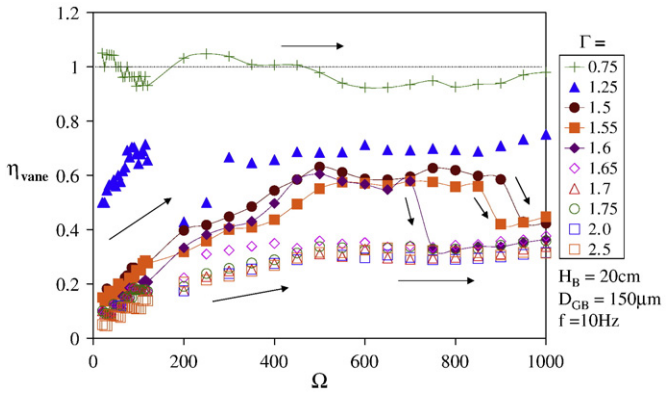

Fig. 3. Dimensionless vane power, η_{vane}, for increasing vane speed, Ω. η_{vane} demonstrates the same characteristic behaviors as P_{vane} in Fig. 2 with $\eta_{vane} \approx 1$ indicating minimal vibration effect and $\eta_{vane} < 1$ indicating the extent of vibration effect. Additionally, η_{vane} is nearly independent of Ω for Ω > 500 rpm, except during bed state transition, indicating that the Ω contribution to bed agitation cancels out.

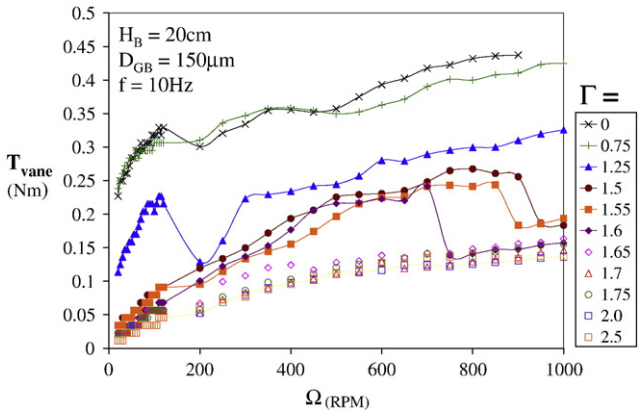

Fig. 5. Vane probe torque, T_{vane}, for increasing vane speed, Ω. T_{vane} for Ω > 200 rpm is calculated from P_{vane} and demonstrates the similar behavior to P_{vane}. Note that torque is not constant for each Γ. T_{vane} dependence on Ω indicates that the vane contributes to the state of the bed.

that the T_{vane} dependence on Ω indicates that the vane contributes to the state of the bed. This behavior is more profound at low Ω.

Fig. 6 focuses on T_{vane} for low Ω measured using vane setup 2 (inset) and the dynamic zero shear rate torque, T_0, that can be extrapolated from this data. The bed is in a quasi-static state when T_0 is a finite positive value, which approaches zero upon transition to the vibro-fluidized state. The behavior of T_0 is analogous to P_{vane}, η_{vane} and the average η_{vane} for Ω > 500 rpm discussed above. Vibration has little effect for Γ < 1 and T_0 is a strong function of Γ for 1 < Γ < 1.6. Upon vibro-fluidization, there is an absence of T_0 for Γ > Γ_c. This is in remarkable agreement with observed granular state behavior using vane setup 1.

Although many studies have employed torque and power measurements from impellers in a granular bed [21,22,64–66], it appears that the only published study combining a vane rheometer with vibration in a deep granular bed without gas fluidization was published by Barois-Cazenave et al. [67]. Using a fixed vertical amplitude, 2 mm, positive displacement vibration source at a frequency of 10 Hz, they show relatively constant viscosity calculated from torque for stress levels up to almost 10^3 Pa. Their analysis ignores observed bed state transitions at stress levels above 10^3. Unfortunately, it is not possible to make a direct comparison between the studies because the study was performed in a shallower bed than the present paper. The bed depth likely affects the power measurements and the occurrence of transitions.

3.2. Power, torque and bed state transitions for increasing Γ

The bed state experiments reported above were repeated for increasing dimensionless vibration acceleration, Γ, at constant vane speed, Ω, instead of increasing Ω while holding Γ constant. The results are shown in Figs. 7–9 for P_{vane}, η_{vane} and T_{vane}, respectively. The same general observations found above for increasing Ω are repeated for increasing Γ. The highest P_{vane}, η_{vane} and T_{vane} are observed for the quasi-static state where Γ < 1. The bed state remains quasi-static for 1 < Γ < Γ_c, however, P_{vane}, η_{vane} and T_{vane} are strong functions of Γ. The bed state transition to vibro-fluidization occurs at the $\Gamma_c \approx 1.6$ inflection point where P_{vane}, η_{vane} and T_{vane} changes from a strong function of Γ to a weak function of Γ. For lower rotation rates, the transition to a vibro-fluidized state at Γ_c is smooth, indicating that granular bed state transition detection is not likely using the vane probe. At high rotation

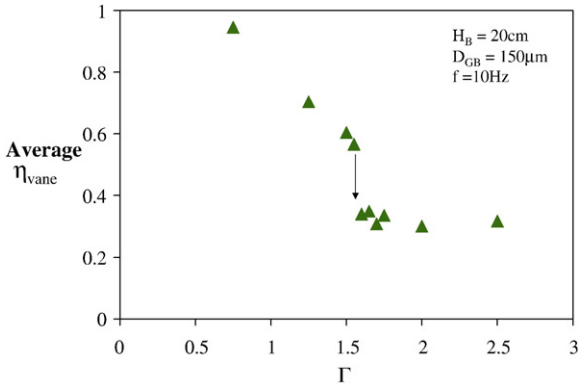

Fig. 4. The dimensionless vane power, η_{vane}, in Fig. 3 is a much weaker function of Ω above 500 rpm. The average η_{vane}, are plotted vs. the dimensionless vibration acceleration, Γ, above. The quasi-static and vibro-fluidized bed states demonstrate the same behaviors for average η_{vane} vs. Γ that were previously shown for η_{vane} vs. Ω.

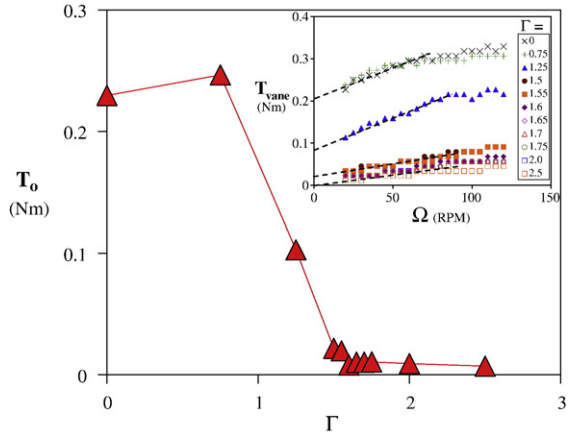

Fig. 6. Vane probe torque, T_{vane}, for increasing vane speed, Ω and extrapolated zero-shear rate torque, T_0, for each dimensionless vibration acceleration, Γ. T_{vane} is measured directly using a torque arm and force gauge because this method is more accurate at low Ω than power measurements. The inset graph shows the low Ω data used to extrapolate the dynamic zero-shear rate torque, T_0, for each Γ. The behavior of T_0 is analogous to P_{vane}, η_{vane} and the average η_{vane} for Ω > 500 rpm discussed above.

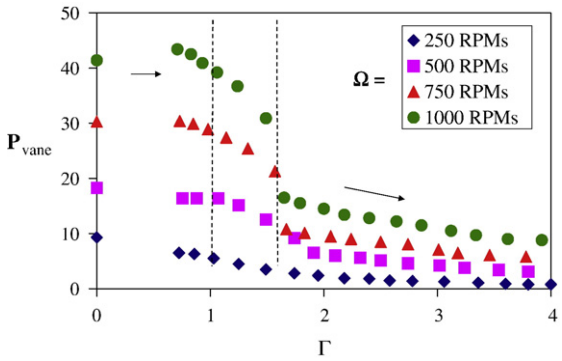

Fig. 7. Vane probe power draw, P_{vane}, for increasing dimensionless vibration acceleration, Γ. The granular bed state behavior shown by P_{vane} for Γ increase is similar to Ω increase in Fig. 2.

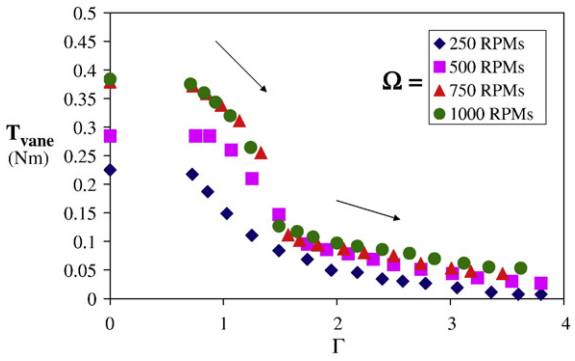

Fig. 9. Vane probe torque, T_{vane}, for increasing dimensionless vibration acceleration, Γ. The granular bed state behavior shown by T_{vane} for Γ increase is similar to Ω increase in Fig. 5.

rates, a smooth change from $0.75<\Gamma<1.6$ is followed by an inflection point around $\Gamma_c=1.6$. One may speculate that the smooth change region is indicative of bed dilation in the quasi-static state that progressively reduces force chain strength or breaks a limited number of force chains due to the influence of vibration. The inflection point around $\Gamma_c=1.6$ results from sudden breakage of all force chains and transition to a vibro-fluidized state. Note that in Fig. 8, the η_{vane} data for $\Omega=500$, 750 and 1000 rpm collapse for $\Gamma>1$, indicating that η_{vane} is independent of the rotation rate at higher Ω. Fig. 9 demonstrates similar collapse behavior for T_{vane} except for $\Omega=500$ rpm at $\Gamma<1.6$. It is also noted that T_{vane} demonstrates a weak dependence on both Γ and Ω for $\Gamma>1.6$.

3.3. Hysteresis

Granular bed state experiments to resolve the transitions reported thus far have been performed for increasing Ω or Γ. The reason for this methodology is to avoid discrepancies resulting from hysteresis. Fig. 10 illustrates behavior for both progressively increasing and decreasing Γ at $\Omega=750$ rpm. During Γ increase, an inflection point in η_{vane} occurs at the Γ_c, as reported above. The bed is vibrated until a point where spontaneous vibro-fluidization occurs presumably due to destruction of the force chains. We speculate that upon Γ decrease, the force chains are formed by a stochastic process that limits the number of force chains formed at a given Γ, resulting in a smoother decrease in η_{vane}. Similar hysteresis behavior occurs while cycling the rate of rotation, Ω. It is important to note that each data point is recorded for the steady state value at the applied Γ or Ω. Therefore, recorded hysteresis is independent of the rate of change for Γ or Ω.

4. Summary and discussion

This work quantitatively identifies three states; static, quasi-static, and vibro-fluidization, through measurements of power and torque required to rotate a vane located inside a vibrated granular bed. The transitions between states are demonstrated when Ω and Γ are increased. There exists a sharp transition to the liquid-like vibro-fluidized state at a critical vibration acceleration at $\Gamma_c=1.6$. This transition is characterized by a sharp decrease in the power and zero shear-rate torque. The power reduction corresponds to a sharp reduction in the apparent viscosity of the material, while the zero shear-rate torque is a commonly accepted measurement of fluid rheology. Prior to this study, detailed studies of vibro-fluidization have been largely limited to shallow granular beds and/or 2D systems confined by parallel plates.

Like all rheological measurements, a holistic description of the system requires complementary macroscopic measurement and microscopic theory. Although this study does not directly probe the particle-level dynamics, it can be inferred that the transition from static to quasi-static behavior is caused by the breaking of stress chains that support the granular bed. Furthermore, the transition from quasi-static to vibro-fluidization occurs when significant particle rearrangements occur locally, allowing the generation of collective behavior such as shock formation and convective motion. Visual observations at the walls of the container confirm the onset of

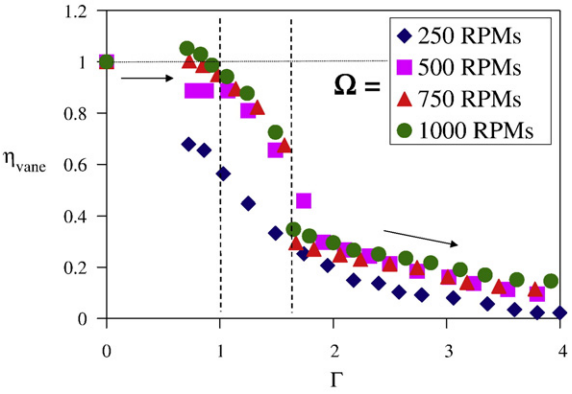

Fig. 8. Dimensionless vane power, η_{vane}, for increasing dimensionless vibration acceleration, Γ. The granular bed state behavior shown by η_{vane} for Γ increase is similar to Ω increase in Fig. 3.

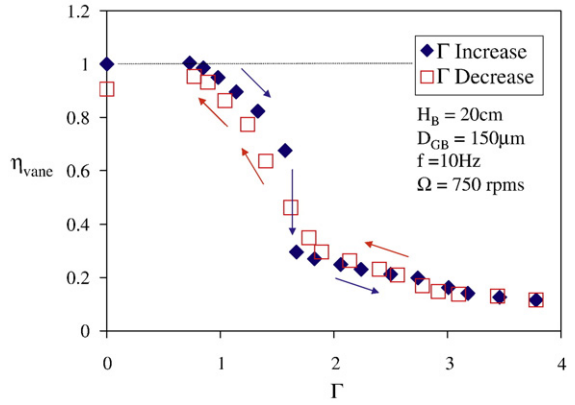

Fig. 10. Dimensionless vane power, η_{vane}, for increasing and decreasing dimensionless vibration acceleration, Γ, at $\Omega=750$ rpm. Hysteresis occurs for increasing vs. decreasing the dimensionless vibration acceleration at constant vane speed.

convection, however the internal dynamics are inaccessible due to the opacity of the material.

Nomenclature

A	Area (m^2)
a_{max}	Maximum acceleration during the vibration cycle (m/s^2)
D_c	Column diameter (cm)
D_{GB}	Glass bead diameter (μm)
f	Vibration frequency (Hz)
F	Force (N)
FI	Fluidization index (−)
g	Gravity (m/s^2)
H_B	Granular bed depth (cm)
L	Length (cm)
m	Mass (Kg)
M_B	Granular bed mass (g)
P_{vane}	Vane power (watts)
ΔP	Pressure drop over the bed (Pa)
T_0	Dynamic zero shear rate torque (Nm)
T_{vane}	Vane torque (Nm)
x_{10}	Glass bead diameter of the 0.1 smallest number fraction of tested beads
x_{90}	Glass bead diameter of the 0.9 smallest number fraction of tested beads
x_{max}	Maximum position displacement from center during the vibration cycle (m)

Greek symbols

Γ	Dimensionless vibration acceleration (a_{max}/g)
Γ_c	Critical dimensionless vibration acceleration (a_{max}/g)
η_{vane}	Dimensionless vane power (P_{vane} vibrated/P_{vane} no vibration)
ω	Period (s^{-1}, 2πf/60)
Ω	Vane speed (rpm)

Acknowledgements

The authors gratefully acknowledge the graduate student support provided by Merck & Co., Inc. We would also like to thank Dr. N. Duke Perreira for his help with the vibration system design used in this paper.

References

[1] C.S. Campbell, Granular Material Flows — an Overview, Powder. Technol. 162 (2006) 208–229.
[2] S.B. Savage, The mechanics of rapid granular flows, in: J.W. a. W. Hutchinson, T.Y. (Eds.), Advances in Applied Mechanics, Academic Press, Inc., Orlando, 1984, pp. 289–366.
[3] J. Duran, Sands, Powders, and Grains: An Introduction to the Physics of Granular materials, Springer, New York, 2000.
[4] B. Cambou, Behavior of Granular Materials, Springer Wien NewYork, New York, NY, 1998.
[5] A. Mehta, Granular Matter: An Interdisiplinary Approach, Springer-Verlag, New York, NY, 1994.
[6] C.E. Brennan, S. Ghosh, C.R. Wassgren, Vertical oscillation of a bed of granular material, Trans. ASME. 63 (1996) 156–160.
[7] A.W. Jenike, Storage and flow of solids, Bull. Univ. Utah 53 (26) (1964) Bulletin Number 123 of the Utah Engineering Experimental Station.
[8] S.B. Savage, M. Sayed, Stresses developed by dry cohesionless granular materials sheared in an annular shear cell, J. Fluid. Mech. 142 (1984) 391–430.
[9] I. Albert, P. Tegzes, R. Albert, J. Sample, A.L. Barabási, T. Vicsek, B. Kahng, P. Schiffer, An experimental study of the fluctuations in granular drag, Materials Research Society, Spring Conference, The Granular State Symposium, MRS, San Fransisco, CA, 2000.
[10] E. Apicella, M. D'Amore, G. Tardos, R. Mauri, Onset of instability in sheared gas fluidized beds, AIChE. J. 43 (5) (1997) 1362–1365.
[11] K.H. de Haas, D. van den Ende, C. Blom, E.G. Altena, G.J. Beukema, J. Mellema, A counter-rotating couette apparatus to study deformation of a sub-millimeter sized particle in shear flow, Rev. Sci. Instr. 69 (3) (1998) 1391–1397.
[12] D. Howell, R.P. Behringer, C. Veje, Stress fluctuations in a 2D granular couette experiment: a continuous transition, Phys. Rev. Let. 82 (26) (1999) 5241–5244.
[13] D. Howell, R.P. Behringer, C. Veje, Fluctuations in granular media, Chaos 9 (3) (1999) 559–572.
[14] R. Khosropour, J. Zirinsky, H.K. Pak, R.P. Behringer, Convection and size segregation in a couette flow of granular material, Phys. Rev. E 56 (4) (1997) 4467–4473.
[15] S.L. Conway, Instability and segregation of particulate materials in bounded shear flows, Chemical and Biochemical Engineering Department, Rutgers, The State University of New Jersey, New Brunswick, NJ., 2004, p. 230.
[16] G. D'Anna, Mechanical properties of granular media, including snow, investigated by a low-frequency forced torsion pendulum, Phys. Rev. E 62 (1) (2000) 982–992.
[17] G. D'Anna, G. G., Vibration-induced jamming transition in granular media, Phys. Rev. E 64 (011306) (2001) 1–6.
[18] G. D'Anna, P. Mayor, A. Barrat, V. Loreto, F. Nori, Observing brownian motion in vibration-fluidized granular matter, Nature 424 (2003) 909–912.
[19] P. Mayor, G. D'Anna, A. Barrat, V. Loreto, Observing brownian motion and measuring temperatures in vibration-fluidized granular matter, New. J. Phys. 7 (28) (2005).
[20] C.V. Navaneethan, S. Missaghi, R. Fassihi, Application of powder rheometer to determine powder flow properties and lubrication efficiency of pharmaceutical particulate systems, AAPS. PharmSciTech. 6 (3) (2005) E398–404.
[21] P.C. Knight, J.P.K. Seville, A.B. Wellm, T. Instone, Prediction of impeller torque in high shear powder mixers, Chem. Eng. Sci. 56 (2001) 4457–4471.
[22] P.J. Sirois, G.D. C., Scaleup of a high-shear granulation process using a normalized impeller work parameter, Pharm. Dev. Tech. 5 (3) (2000) 365–374.
[23] A. Lekhal, S.L. Conway, B.J. Glasser, J.G. Khinast, Characterization of granular flow of wet solids in a bladed mixer, AIChE. J. 52 (8) (2006) 2757–2766.
[24] C.R. Wassgren, C.E. Brennan, M.L. Hunt, Vertical vibration of a deep bed of granular material in a container, Trans. ASME. 63 (1996) 712–719.
[25] J.R. de Bruyn, B.C. Lewis, M.D. Shattuck, H.L. Swinney, Spiral patterns in oscillated granular layers, Phys. Rev. E 63 (041305) (2001) 1–12.
[26] D.I. Goldman, J.B. Swift, H.L. Swinney, Noise, coherent fluctuations, and the onset of order in an oscillated granular fluid, Phys. Rev. Let. 92 (17) (2004) 174302.
[27] B. Thomas, M.O. Mason, Y.A. Lui, A.M. Squires, Identifying states in shallow vibrated beds, Powder. Technol. 57 (1989) 267–280.
[28] S. Luding, E. Clément, A. Blumen, J. Rajchenback, J. Duran, Studies of columns of beads under external vibrations, Phys. Rev. E 49 (2) (1994) 1634–1646.
[29] S.B. Savage, Streaming motions in a bed of vibrationally fluidized dry granular material, J. Fluid. Mech. 194 (1988) 457–478.
[30] Q.D. Nguyen, D.V. B., Yield stress measurement for concentrated suspensions, J. Rheol. 27 (4) (1983) 321–349.
[31] Standard Test Method for Field Vane Shear Test in Cohesive Soil, in D2573-01, ASTM International, 2001.
[32] Standard Test Method for Laboratory Miniature Vane Shear Test for Saturated Fine-Grained Clayey Soil, in D 4648-05, ASTM International, 2005.
[33] J.L. Briggs, J.F. Steffe, Z. Ustunol, Vane method to evaluate the yield stress of frozen ice cream, J. Dairy. Sci. 79 (1996) 527–531.
[34] D.B. Genovese, M.A. R., Vane yield stress of starch dispersions, J. Food. Sci. 68 (7) (2003) 2295–2301.
[35] A. Tárrega, E. Costell, M.A. Rao, Vane yield stress of native and cross-linked starch dispersions in skimmed milk: effect of starch concentration and ë-carrageenon addition, Food. Sci. Tech. 12 (3) (2006) 253–260.
[36] V.D. Truong, C.R. Daubert, M.A. Drake, S.R. Baxter, Vane reometry for textural characterization of cheddar cheeses: correlation with other instrumental and sensory measurements, Leensm.-Wiss. u.-Technol. 35 (2002) 305–314.
[37] J. Duran, T. Mazozi, E. Clement, J. Rajchenbach, Decompaction modes of a two-dimensional "sandpile" under vibration: model and experiments, Phys. Rev. E 50 (4) (1994) 3092–3099.
[38] J.M. Huntley, Fluidization, segregation and stress propagation in granular materials, Phil. Trans. Math,. Physical. and. Eng. Sci. 356 (1747) (1998) 2569–2590.
[39] C.H. Tai, S.S. H., Dynamic behaviors of powders in a vibrating bed, Powder. Technol. 139 (2004) 221–232.
[40] S.C. Yang, S.S. H., Self-diffusion analysis in a vibrated granular bed, Adv. Powder. Tech. 12 (1) (2001) 61–77.
[41] C. Bizon, M.D. Shattuck, J.B. Swift, Linear stability analysis of a vertically oscillated granular layer, Phys. Rev. E 60 (6) (1999) 7210.
[42] E. Clément, L. Vanel, J. Rajchenbach, J. Duran, Pattern formation in a vibrated granular flow, Phys. Rev. E 53 (3) (1996) 2972–2975.
[43] G.B. Lubkin, Oscillating Granular Layer Produce Stripes, Squares, Hexagons… Physics Today, October 1995, pp. 17–19.
[44] S.J. Moon, J.B. Swift, H.L. Swinney, Role of friction in pattern formation in oscillated granular layers, Phys. Rev. E 69 (031301) (2004) 1–6.
[45] P.B. Umbanhowar, H.L. S., Wavelength scaling and square/stripe and grain mobility transitions in vertically oscillated granular layers, Physica A 288 (2000) 344–362.
[46] R.D. Wildman, J.M. H., Novel method for measurement of granular temperature distributions in two-dimensional vibro-fluidised beds, Powder Technol. 113 (2000) 14–22.
[47] H. Takahashi, A. Suzuki, T. Tanaka, Behaviour of a particle bed in the field of vibration: i. analysis of particle motion in a vibrating vessel, Powder Technol. 2 (1968/69) 65–71.
[48] M.L. Hunt, S.S. Hsiau, K.T. Hong, Particle mixing and volumetric expansion in a vibrated granular bed, J. Fluids Eng. 116 (1994) 785–791.
[49] S. Klongboonjit, The Effects of Particle Elasticity on the Convection in Deep Vertically Shaken Particle Beds, in Dept. Mechanical Engineering, University of Southern California, Los Angeles, CA, 2005, p. 175.
[50] G. Rátkai, Particle flow and mixing in vertically vibrated beds, Powder Technol. 15 (1976) 187–192.
[51] P. Sistla, O. Baran, Q. Chen, P.H. Poole, R.J. Martinuzzi, Bulk motion of granular matter in an agitated cylindrical bed, Phys. Rev. E 71 (011303) (2005) 1–11.
[52] E.E. Ehrichs, H.M. Jaeger, G.S. Karczmar, J.B. Knight, V.Y. Kuperman, S.R. Nagel, Granular convection observed by magnetic resonance imaging, Science 267 (5204) (1995) 1632–1634.

[53] H.M. Jaeger, S.R. Nagel, R.P. Behringer, Granular solids, liquids, and gases, Rev. Modern Phys. 68 (4) (1996) 1259–1273.
[54] E.E. Ehrichs, J.K. Flint, H.M. Jaeger, J.B. Knight, S.R. Nagel, G.S. Karczmar, V.Y. Kuperman, Convection in vertically vibrated granular materials, Phil. Trans.: Math, Physical and Eng. Sci. 356 (1747) (1998) 2561–2567.
[55] K. Godard, J.F. R., The use of slow speed stirring to initiate particulate fluidisation, Chem. Eng. Sci. 24 (1969) 194–195.
[56] R.H. Nielsen, N. Harnby, T.D. Wheelock, Mixing and circulation in fluidized beds of flour, Powder Technol. 32 (1982) 71–86.
[57] E. Marring, A.C. Hoffmann, L.P.B.M. Janssen, The effect of vibration on the fluidization behaviour of some cohesive powders, Powder Technol. 79 (1994) 1–10.
[58] J.R. Wank, S.M. George, A.W. Weimer, Vibro-fluidization of fine boron nitride powder at low pressure, Powder Technol. 121 (2001) 195–204.
[59] Y. Mawatari, T. Ikegami, Y. Tatemoto, K. Noda, Prediction of agglomerate size for fine particles in a vibro-fluidized bed, J. Chem. Eng. Jpn. 36 (3) (2003) 277–283.
[60] Y. Mawatari, T. Koide, Y. Tatemoto, T. Takeshita, K. Noda, Comparison of three vibrational modes (twist, vertical and horizontal) for fluidization of fine particles, Adv. Powder Tech. 12 (2) (2001) 157–168.
[61] G. Metcalfe, S.G.K. Tennakoon, L. Kondic, D.G. Schaeffer, R.P. Behringer, Granular Friction, Coulomb Failure, and the Fluid-Solid Transition for Horizontally Shaken Granular Materials, 2000.
[62] S.G.K. Tennakoon, L. Kondic, R.P. Behringer, Onset of flow in a horizontally vibrated granular bed: convection by horizontal shearing, Europhys. Lett. 45 (4) (1999) 470–475.
[63] N.J.M. Kuipers, E.J. Stamhuis, A.A.C.M. Beenackers, Fluidization of potato starch in a stirred vibrating fluidized bed, Chem. Eng. Sci. 51 (11) (1996) 2727–2732.
[64] P. Holm, T. Schaefer, H.G. Kristensen, Granulation in high-speed mixers: part V. Power consumption and temperature changes during granulation, Powder. Technol. 43 (1985) 213–223.
[65] P. Holm, T. Schaefer, H.G. Kristensen, Granulation in high-speed mixers: part VI. Effects of process conditions on power consumption and granule growth, Powder. Technol. 43 (1985) 225–233.
[66] A.B. Wellm, Investigation of a High Shear Mixer/Agglomerator, in School of Chemical Engineering, University of Birmingham, Birmingham, UK., 1997, p. 316.
[67] A. Barois-Cazenave, P. Marchel, V. Falk, L. Choplin, Experimental study of powder rheological behavior, Powder. Technol. 103 (1) (1999) 58–64.